JEM Journal of Experimental Medicine

ARTICLE

Tingible body macrophages arise from lymph node–resident precursors and uptake B cells by dendrites

Neta Gurwicz[1], Liat Stoler-Barak[1], Niklas Schwan[2], Arnab Bandyopadhyay[2], Michael Meyer-Hermann[2,3], and Ziv Shulman[1]

Antibody affinity maturation depends on the formation of germinal centers (GCs) in lymph nodes. This process generates a massive number of apoptotic B cells, which are removed by a specialized subset of phagocytes, known as tingible body macrophages (TBMs). Although defects in these cells are associated with pathological conditions, the identity of their precursors and the dynamics of dying GC B cell disposal remained unknown. Here, we demonstrate that TBMs originate from pre-existing lymph node–resident precursors that enter the lymph node follicles in a GC-dependent manner. Intravital imaging shows that TBMs are stationary cells that selectively phagocytose GC B cells via highly dynamic protrusions and accommodate the final stages of B cell apoptosis. Cell-specific depletion and chimeric mouse models revealed that GC B cells drive TBM formation from bone marrow–derived precursors stationed within lymphoid organs prior to the immune challenge. Understanding TBM dynamics and function may explain the emergence of various antibody-mediated autoimmune conditions.

Introduction

Activation of the adaptive immune response by vaccination or invading microbes is essential for effective pathogen clearance and the establishment of long-lasting immunological memory. Effective immunity is mediated by antibodies that prevent pathogen invasion into the host, and memory cells that respond rapidly during recurrent exposures (Shlomchik and Weisel, 2012). Naive B cells that carry a pathogen-specific B cell antigen receptor (BCR) rapidly proliferate in lymphoid organs in response to vaccination or pathogen infection and can either differentiate into antibody-secreting cells, memory cells, or enter the germinal center (GC) reaction (Victora and Nussenzweig, 2012; Glaros et al., 2021; Grenov et al., 2022). Within GCs, B cells proliferate and improve the affinity of their BCRs through the insertion of somatic hypermutations (SHMs) into their immunoglobulin genes. Since this process is random, it can also introduce determinantal mutations and lead to apoptosis-mediated cell death through the generation of frameshifts and stop codons in the immunoglobulin genes (Stewart et al., 2018; Mayer et al., 2017; Muramatsu et al., 2000). On rare occasions, mutations are introduced into non-BCR genes which can also trigger cell death in GC B cells (Hasham et al., 2012; Zaheen and Martin, 2011). SHMs primarily occur in a dense part of the GC, known as the dark zone (DZ), whereas the selection of B cells carrying improved BCR variants by helper T cells takes place in the less-crowded region of the GC, located closer to the LN capsule and known as the light zone (LZ; Allen et al., 2004). GC B cells that do not receive sufficient T cell help or other survival signals in the LZ also die by apoptosis (Biram and Shulman, 2020; Mayer et al., 2017; Stewart et al., 2018; Peperzak et al., 2012). Although GC structures accommodate extensive apoptosis events in both the DZ and LZ throughout their lifetime (Mayer et al., 2017), the accumulation of dead cells within the GC structures does not occur under nonpathological conditions (Liu et al., 1989, 1991).

Clearance of apoptotic and defective B cells within the GC is carried out by phagocytic histiocytes known as tingible body macrophages (TBMs; Bellomo et al., 2018; Swartzendruber and Congdon, 1963). These big cells were described by Flemming more than 100 yr ago as large phagocytic cells containing degraded lymphocytes or condensed apoptotic nuclei referred to as "tingible bodies" (Swartzendruber and Congdon, 1963; Flemming, 1884; Sminia et al., 1983; Hofman et al., 1984). In

[1]Department of Systems Immunology, Weizmann Institute of Science, Rehovot, Israel; [2]Department of Systems Immunology and Braunschweig Integrated Centre of Systems Biology, Helmholtz Centre for Infection Research, Braunschweig, Germany; [3]Institute for Biochemistry, Biotechnology and Bioinformatics, Technische Universität Braunschweig, Braunschweig, Germany.

Correspondence to Ziv Shulman: ziv.shulman@weizmann.ac.il.

lymphoid organs, these cells typically reside in the DZ, although occasionally, they are detected in the GC LZ next to follicular dendritic cells (FDCs; Kranich et al., 2008; Wittenbrink et al., 2011). TBMs express typical myeloid markers including CD68 and CX3CR1, but lack the commonly expressed macrophage marker F4/80 (Bellomo et al., 2021; Rabinowitz and Gordon, 1991; Wittenbrink et al., 2011; Kranich et al., 2008). Membranal phosphatidylserines (PS) are the hallmark of cells undergoing apoptosis and specific types of macrophages, including TBMs, express and bind multiple PS-binding adaptors and receptors, such as MFGE8 and MERTK (Rahman et al., 2010; Bratton and Henson, 2008; Lemke, 2019), and engulfment-promoting molecules such as Tim-4 (Wong et al., 2010). Rapidly removing the dying cells by phagocytes is critical, since intracellular material can trigger unwanted immune cell activation and the formation of poly- or self-reactive antibodies (Nagata et al., 2010; Savill et al., 2002; Khan et al., 2013; Carroll, 2000; Degn et al., 2017). Indeed, lack of TBMs or defects in their functions were associated with autoantibody production and autoimmune diseases such as systemic lupus erythematosus (Hanayama et al., 2004; Baumann et al., 2002; Nagata et al., 2010; Rahman et al., 2010; Vinuesa et al., 2009; Gaipl et al., 2005). Yet, the biological process of apoptotic cell removal and its dynamics in the GC has not been documented.

Several studies examined B cell death in the GC, and measurement of GC size, B cell proliferation, and apoptosis suggest that 50% of the GC B cells die every 5 h (Mayer et al., 2017). Thus, as cells that surveil the GC, removing dead cells, TBMs face an enormous challenge. How TBMs cope with these extensive death events and prevent the accumulation of deleterious self-antigens and debris in the GC structure remains unknown. Furthermore, despite comprehensive studies regarding the origins and functions of myeloid cell populations in lymphoid and non-lymphoid organs (Bellomo et al., 2018; Park et al., 2022), little is known regarding the cellular origin of TBMs. Here, we show that TBMs originate from LN-resident precursors that enter the follicles in a GC-dependent manner and scavenge apoptotic cells through a "stand hunting" strategy.

Results

GC-resident macrophages consume B cells through dynamic dendrites

Several populations of macrophages are located within the lymphoid organs in specific niches, yet only a few of these are engaged in phagocytic activity (Bellomo et al., 2018; Guilliams et al., 2020; Martin et al., 2014; Lemke, 2019). To examine the location of LN-resident macrophage populations that consume B cells, we used CX3CR1^{GFP} transgenic mice in which most of the monocytes and macrophages express GFP (Jung et al., 2000). To visualize phagocytic macrophages, transgenic B cells, which are specific for a defined antigen (4-hydroxy-3-nitrophenylacetyl [NP]–specific tdTomato$^+$ B1-8^{hi} B cells), were adoptively transferred into primed CX3CR1^{GFP} host mice followed by boosting with NP-OVA antigen (Schwickert et al., 2009; Shulman et al., 2014). After 7 d, when GCs were formed, popliteal LNs were dissected and scanned by two-photon laser scanning microscopy (TPLSM; Shulman et al., 2013). This approach revealed three well-defined niches in which CX3CR1-expressing macrophages reside in the B cell zone of the LN, including cells next to the LN capsule, known as subcapsular sinus macrophages (SSMs; Carrasco and Batista, 2007; Gray and Cyster, 2012; Phan et al., 2007), cells located in GCs known as TBMs (Smith et al., 1998), and an additional undefined rare subpopulation located throughout the LN follicles but not within the subcapsular sinus or GCs (Fig. 1 A). Thus, although many antigen-specific B cells were scattered throughout the LN follicles and next to the LN capsule, intracellular B cells were observed only within GC-resident macrophages.

To examine the dynamics and specificity of GC-resident macrophages, CX3CR1-expressing cells within the LN cortex were imaged by intravital live imaging combined with TPLSM. This analysis revealed that GC-resident macrophages are stationary cells, while GC B cells rapidly move within the GC structure (Fig. 1, A and B; and Video 1). Direct imaging of GC structures revealed two types of CX3CR1-expressing phagocytic cells; one that consumes B cells within the GC niche (64.8% of the cells) and an additional subset located at the margins of the GC structures (35.2% of the cells; Video 2, Video 3, and Video 4). Since TPLSM effectively penetrates the LN cortex, we could enumerate the absolute number of TBMs per GC structure. The range of TBMs per whole GC was between 10 and 40, with an average of 25 cells (Fig. 1 C). Furthermore, intravital imaging revealed that GC-resident macrophages contained up to 12 detectable tdTomato$^+$ B cells (4.18 ± 2.7 B cells on average in 71 analyzed macrophages containing at least 1 B cell, range 1–12), and continuously consumed cells primarily through uptake by long and dynamic protrusions (Video 2, Video 3, and Video 4). The rate of B cell consumption by TBMs was one cell per 10 min on average, and each phagocytic event lasted 13.4 min on average (Fig. 1, D and E). Thus, we conclude that TBMs are stationary cells that repeatedly initiate the phagocytic process of GC B cells through highly dynamic protrusions.

The intravital imaging experiments revealed that TBMs rapidly consume B cells located in their near proximity. This observation raised the possibility that GC macrophages selectively consume GC B cells, or alternatively, they uptake cells randomly. It was previously shown that naive B cells frequently enter the GC structure (Schwickert et al., 2007; de Carvalho et al., 2022; Hägglöf et al., 2022). To examine if TBMs specifically take up GC B cells, we adoptively transferred into mice a large number of tdTomato$^+$ naive B cells at the peak of the GC response, followed by intravital imaging. As expected, naive B cells entered the GC and occasionally interacted with GC macrophages; however, we did not detect any events in which TBM consumed a naive B cell (Fig. 1, D–F). Within the GC, T and GC macrophages have been detected in both the LZ and the DZ, indicating that interaction between these cells might occur (Wittenbrink et al., 2011). To examine whether TBMs can take up T follicular helper (Tfh) cells, we transferred OVA-specific tdTomato$^+$ OT-II T cells into mice prior to OVA immunization. These cells differentiated into GC-resident Tfh cells after NP-OVA boosting, as previously shown (Shulman et al., 2014). In analogy to the naive B cells, intravital imaging did not detect

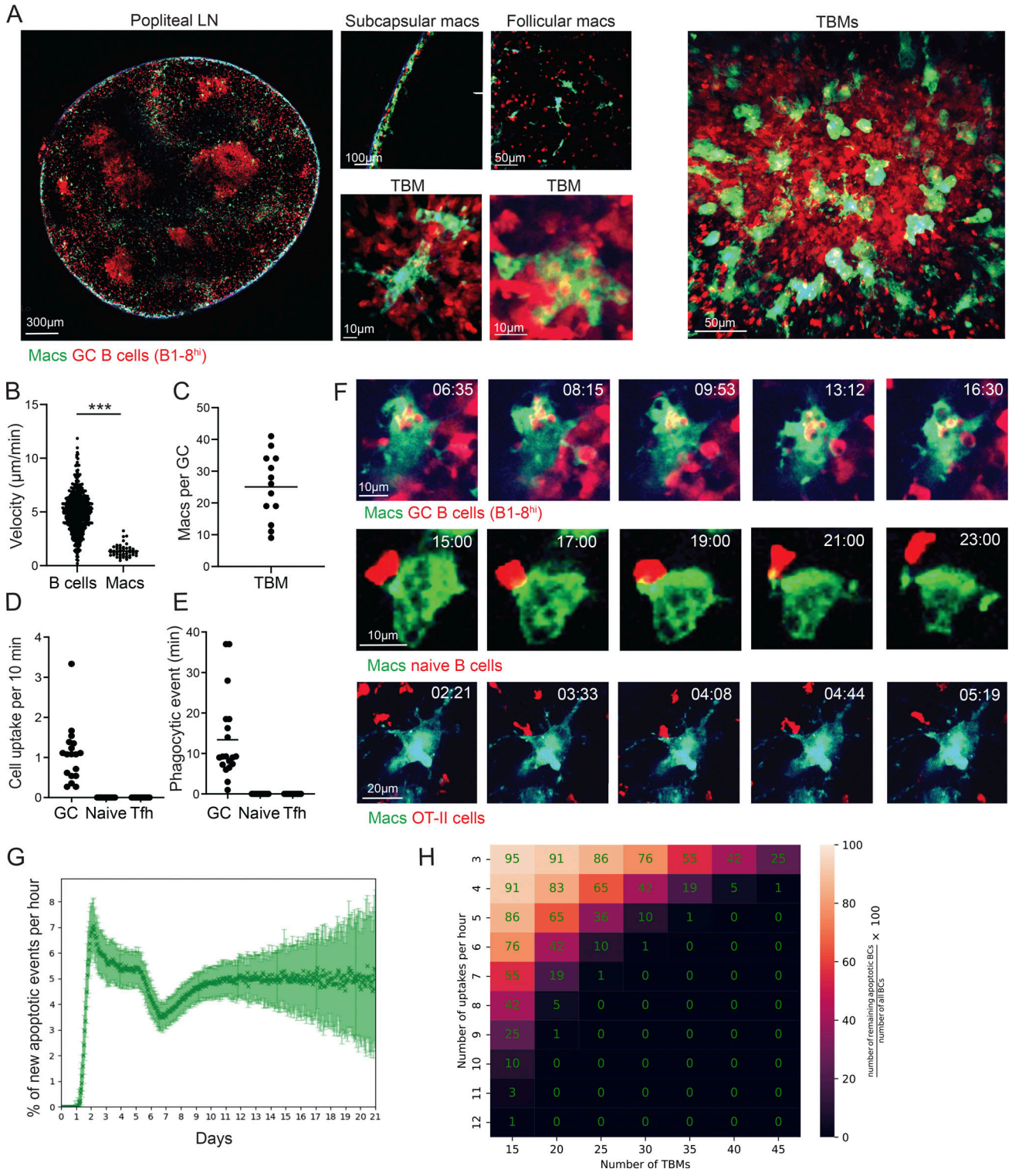

Figure 1. **B cell disposal in GCs is mediated by TBMs through highly dynamic dendrites. (A)** TPLSM images of popliteal LNs of OVA-primed CX3CR1^{GFP} mice that received TdTomato^{+} B1-8^{hi} B cells, 7 d after intra-footpad NP-OVA boost. **(B)** Velocity of B cells and TBMs in the GC. Each dot represents a single cell. **(C)** Number of macrophages in the GCs. Each dot represents a GC; three mice were imaged. **(D and E)** OVA-primed CX3CR1^{GFP} mice that received either TdTomato^{+} B1-8^{hi} B cells prior to boosting, naive B cells 1 d before TPLSM intravital imaging, or TdTomato^{+} OT-II T cells prior to initial immunization. TPLSM intravital imaging was performed 7 d after intra-footpad boost with NP-OVA. Number of cells (D) and cell uptake rate per single TBM (E). Each dot represents a single TBM uptake event. The data were obtained from two to three mice. Two-tailed Student's *t* test; ***, $P < 0.0001$; ns, not significant. **(F)** TPLSM images of popliteal LNs of CX3CR1^{GFP} interactions with the transferred lymphocytes. Two to three mice were imaged per condition. **(G)** Simulation of apoptotic B cell number per hour based on previously published GC dynamic modeling. **(H)** Prediction of the number of macrophages required for removal of all of the apoptotic cells in the GC. Number of apoptotic cells = (number of TBMs × uptake rate)/the number of B cells in the GC.

uptake of OT-II T cells by TBMs in GCs (Fig. 1, D–F). Of note, in addition to the adoptively transferred fluorescent cells, there were many invisible host-derived cells in these experiments. Thus, we conclude that TBMs specifically consume GC B cells and do not pick up random cells in their proximity.

Based on the measurement of TBM number per GC and rate of B cell uptake, we performed agent-based modeling studies to estimate the efficiency of GC macrophages in the removal of apoptotic cells. Using an in silico model (Meyer-Hermann, 2021), we found that at the peak of the GC response, 2–4% of the GC B cells are apoptotic (Fig. 1 G), a number that is consistent with previous studies (Stewart et al., 2018; Mayer et al., 2017). To estimate the number of TBMs required to remove all apoptotic cells from the GC, the difference between the number of apoptotic cells and the number of phagocytosed cells was calculated. Based on our dynamic measurements showing uptake of six B cells per TBM per hour, our analysis indicated that 30 TBMs per GC are required to remove all of the dying cells (Fig. 1 H). Using intravital microscopy, we measured 10–40 TBMs per GC structure with an average of 25 (Fig. 1 C). Thus, these experimental and computational analyses indicate that the number of TBMs present per GC is sufficient to remove most of the dying cells.

Macrophage infiltration into LN follicles requires GCs

The TPLSM imaging revealed CX3CR1-expressing cells in three different niches within the LNs of immunized mice, including follicular macrophages consisting of both TBMs and non-GC resident cells. An additional large CX3CR1^{+} cell population that resides in the LNs in close proximity to the B cell follicles is known as T cell zone macrophages (TZMs; Fig. 2 A). To examine if GC B cells drive the invasion of macrophages into the LN follicles, we first visualized CX3CR1-expressing cells in immunized CX3CR1^{GFP} transgenic mice before and after GC formation. For this purpose, tdTomato^{+} B1-8^{hi} B cells were adoptively transferred into CX3CR1^{GFP} host mice followed by immunization with NP-KLH into the hind footpads. TPLSM revealed CX3CR1-expressing cells in the T cell zone of the LNs, and very few GFP^{+} cells were detected in the LN cortex on day 3 after immunization (Fig. 2 A). After an additional 2 d, small clusters of tdTomato^{+} B1-8^{hi} B cells were formed that were associated with phagocytic CX3CR1-expressing cells. On day 7 after immunization, clear GC structures were detected hosting TBMs (Fig. 2 A). The emergence of the GC niche occurring in parallel to the entry of macrophages into the LN follicles suggests that the migration of macrophages into follicles depends on the presence of GC cells.

To quantify the entry of macrophages into the LN follicles and examine whether GCs promote this process, we compared the number of CX3CR1-expressing cells in LN follicles in unimmunized versus immunized mice, as well as in SLAM-associated protein (SAP)–deficient mice, which are unable to form GCs in response to vaccination (Crotty et al., 2003; Cannons et al., 2011). Since macrophages in SAP-deficient mice did not express GFP, we used popliteal and inguinal LN sections stained for CD68 as a marker for macrophages, and IgD as a marker for non-GC B cells. This analysis revealed that unmanipulated mice had very few macrophages in their inguinal and popliteal LN follicles, while LNs from immunized mice showed follicle-resident macrophages (Fig. 2 B). In immunized SAP-deficient mice, infiltration of macrophages into the LN cortex was not detected, suggesting that the GCs, rather than general inflammatory cues, are required to attract these cells into the follicles (Fig. 2 C). We and others previously showed that SAP is not required for GC formation in Peyer's patches (PPs; Biram et al., 2020; Ma et al., 2006). Thus, to examine if indeed the lack of GCs accounted for the lack of macrophage infiltration, or if other SAP-related functions played a role, we examined the follicles of PPs of SAP-deficient mice. As opposed to LNs, the PPs hosted macrophages in their follicles and GC structures (Fig. 2 C). Thus, we conclude that GCs are essential for effective macrophage infiltration into LN follicles during an immune response.

TBMs originate from a precursor pool located within lymphoid organs

Although the origins of SSMs and TZMs were clearly defined, the precursor population of TBMs remains unknown (Bellomo et al., 2018; Guilliams et al., 2020). To examine if the TBMs originate from bone marrow (BM)–derived monocytes or a local LN-resident macrophage cell population, WT host mice were subjected to either full body irradiation or irradiation with shielding of the upper body part to protect the cells within the brachial LNs from local cell death. Both irradiated mice were transplanted with traceable BM cells derived from CX3CR1^{GFP} donors (Fig. 3 A). Imaging of brachial LN and PP histological sections derived from the chimeric immunized mice that were fully exposed to the irradiation revealed that TZM originated from the donor cells, as previously reported (Baratin et al., 2017; Fig. 3 B). To examine the contribution of BM-derived cells to TBMs, LN sections were stained for CD68 and the ratio of GFP (donor cells) to total CD68^{+} cells (donor and host cells) was examined. This analysis revealed that 75% of the TBMs are of BM origin and the rest of the cells might represent irradiation-resistant host-derived cells (Fig. 3, C and F). These experiments demonstrate that TBMs mainly originate from BM-derived cells.

TZM macrophages arrive from the BM of adult mice and occupy the LNs and other organs for long periods (Perdiguero and Geissmann, 2016; Baratin et al., 2017). To examine if TBMs arise from intermediate LN-resident cells such as the TZMs, we used shielded chimeras in which the upper body LNs were protected from irradiation, while the lower BMs and PPs were not shielded from the irradiation followed by the transfer of BM cells from CX3CR1^{GFP} donors (Fig. 3 A). Under these conditions, the LN-resident macrophages are not ablated whereas most of the BM precursors are replaced. In this setting, LN-resident macrophages were CD68^{+} GFP^{-}, whereas most of the BM-derived cells were GFP^{+}. Under this setting, GFP^{+} cells were detected in the T cell zone of the LNs (Fig. 3 D). Close analysis of brachial LNs, which were protected from the irradiation, showed a small fraction of GFP^{+} CD68^{+} cells (18.82% on average) compared with the fully irradiated mice (75% on average), whereas no difference was detected in PPs, which were exposed to the irradiation in the shielded animals (Fig. 3, E and F). These

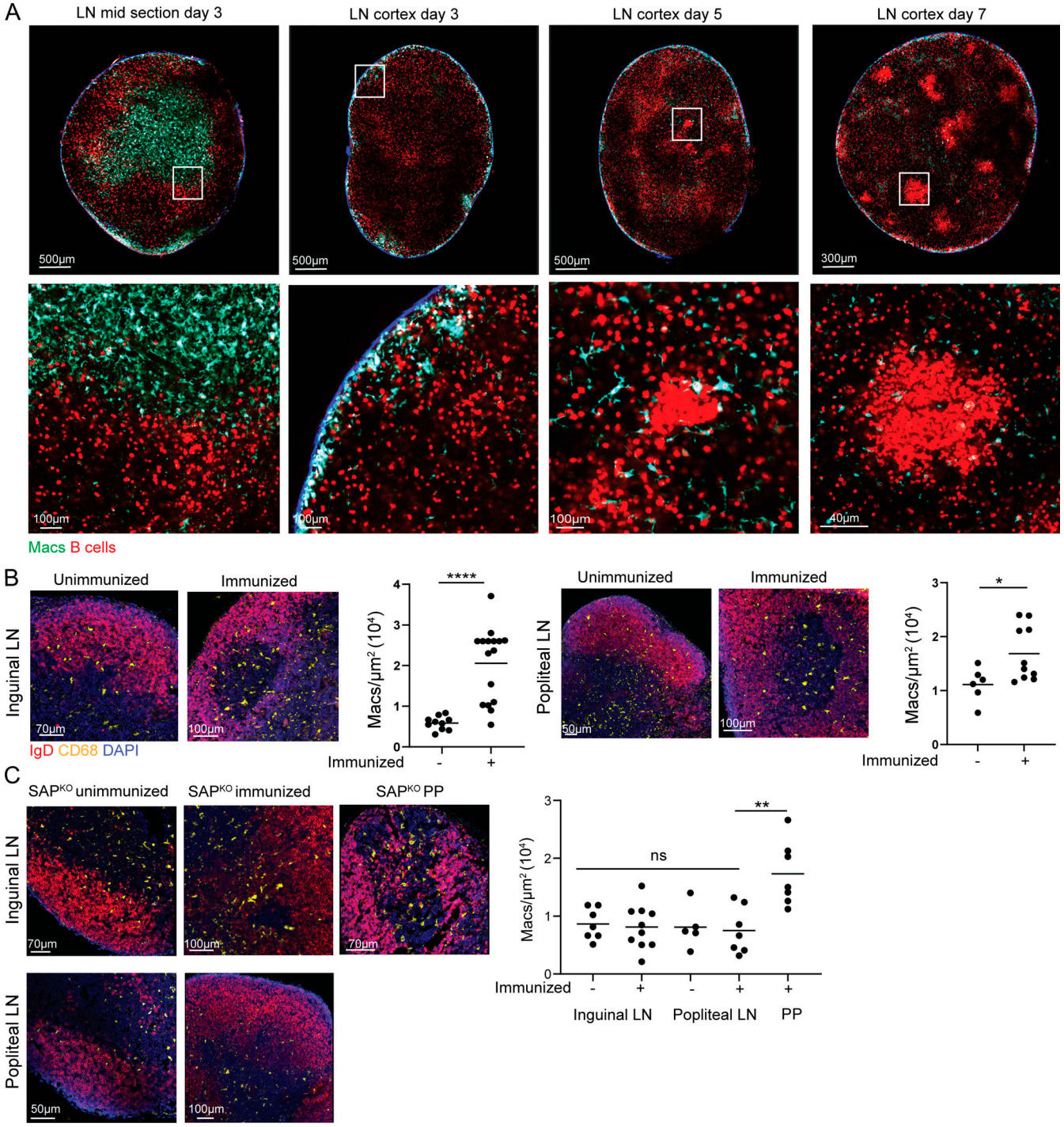

Figure 2. **Macrophage infiltration into LN follicles depends on GCs. (A)** TPLSM images of popliteal LNs derived from CX3CR1^{GFP} mice that were adoptively transferred with TdTomato^{+} B1-8^{hi} B cells and imaged 3, 5, and 7 d after intra-footpad immunization with NP-OVA. Each time point was repeated twice, with two mice in each repeat. **(B)** Immunofluorescence staining of LN-derived from immunized and unimmunized mice. Each dot represents the density of macrophages in LN follicles; three to four mice were analyzed from each group. **(C)** Immunofluorescence staining of LNs derived from unimmunized and immunized SAP^{KO} mice. Each dot represents the density of macrophages in the follicles of three mice. Line represents the mean. *, P < 0.05; *, P < 0.01; ****, P < 0.0001; ns, not significant. Two-tailed Student's *t* test in B, one-way ANOVA in C.

findings demonstrate that TBMs originate from an LN-resident pool of long-lived precursors, established from BM-derived cells before immunization. Since TZMs show similar migration and persistence patterns (Baratin et al., 2017), these data favor the possibility that TZMs are the precursors of the TBMs.

TBMs do not differentiate from subcapsular macrophages

In addition to TBMs, the SSMs constitute a large macrophage population that is located very close to the GCs and interacts with B cells (Bellomo et al., 2018, 2021; Suan et al., 2015; Phan et al., 2009). The hallmark of the former is the expression of

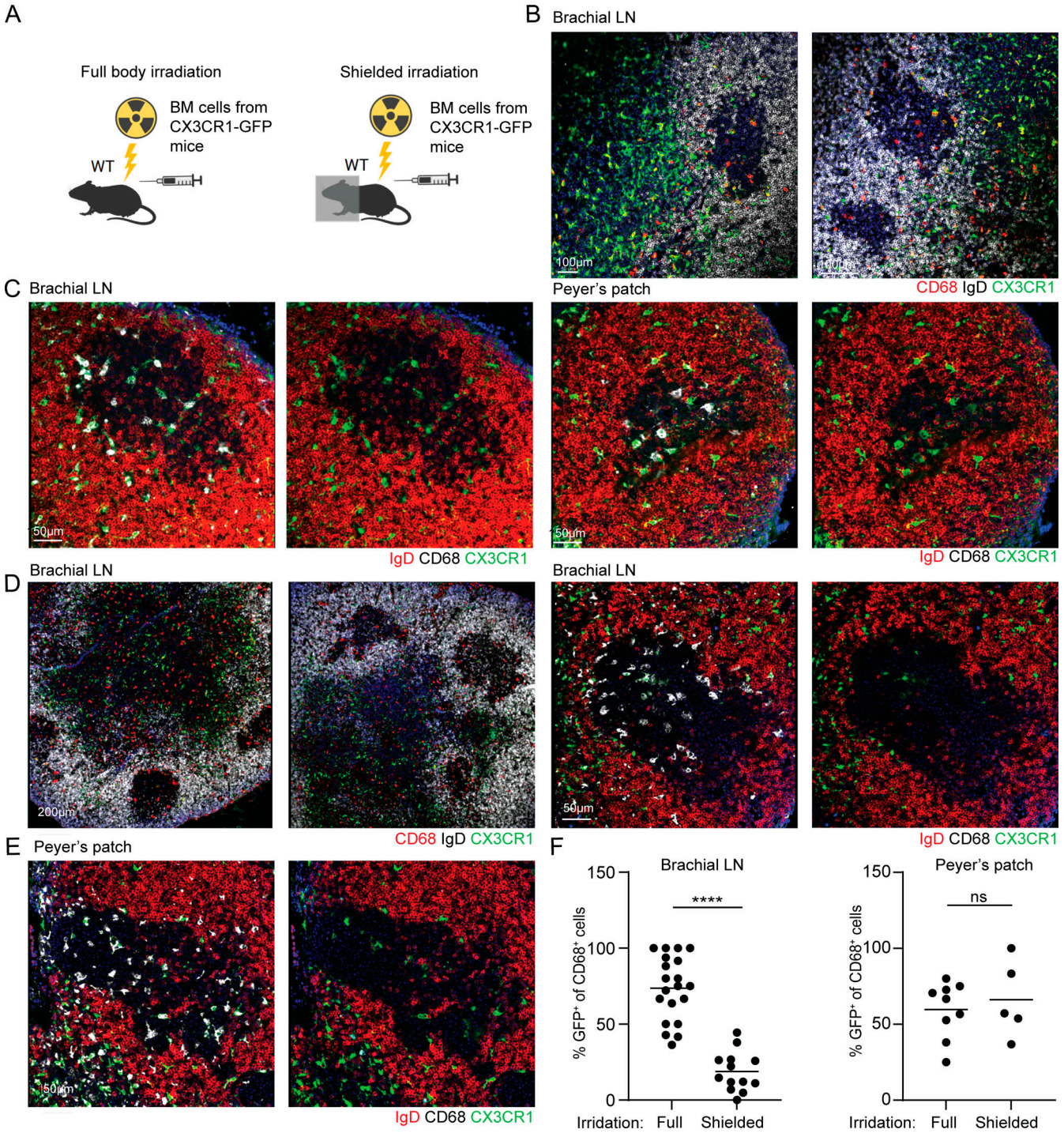

Figure 3. **TBMs originate from LN-resident precursors. (A)** Scheme of chimeric mouse production. **(B and C)** Immunofluorescence staining of brachial LNs and PPs of fully irradiated chimeric mice. **(D and E)** Immunofluorescence staining of brachial LNs and PPs derived from shielded chimeric mice. **(F)** Quantification of $CD68^+$ GFP^+ to $CD68^+$ cells ratios. Each dot represents the ratio in a single GC. Four mice were analyzed in two independent experiments. Line represents the mean. ****, $P < 0.0001$; ns, not significant; two-tailed Student's *t* test.

CD169, also known as Siglec-1, which is not expressed by TZMs (Mondor et al., 2019). To examine if these cells can differentiate into TBMs, $CD169^{DTR}$ mice were immunized to initiate an immune response and allow antigen delivery by SSM into the LNs, followed by $CD169^+$ cell depletion using diptheria toxin (DT) treatment on days 2, 4, and 6 after immunization (Fig. 4 A). This protocol was used to avoid defects in SSM-mediated antigen delivery into the LNs during the initiation of the immune response. 1 d after the final DT injection, inguinal and popliteal LNs were removed to ensure the ablation of the SSMs by flow cytometry and by immunofluorescence staining (Fig. 4, B and C). Analysis of GC macrophages by CD68 staining showed a similar

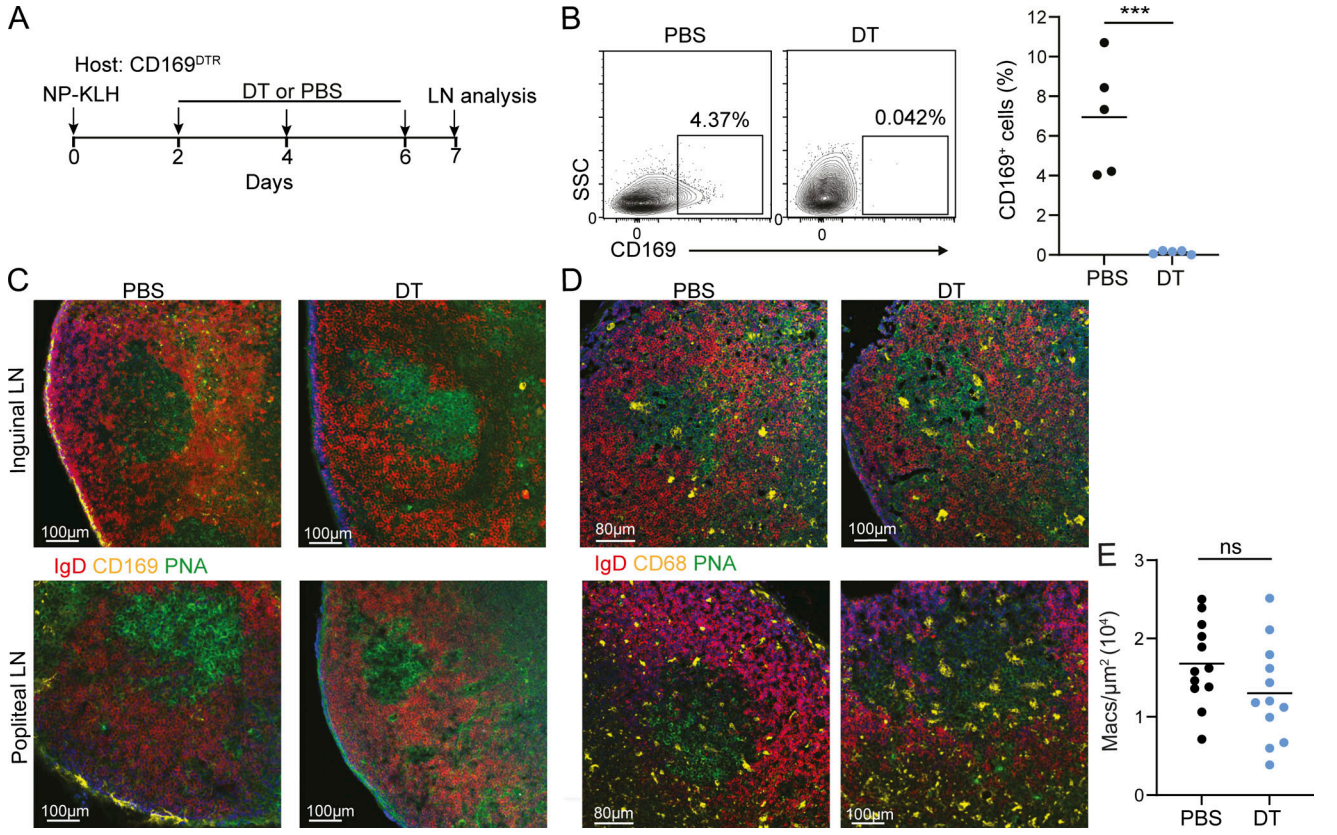

Figure 4. **Subcapsular macrophages do not give rise to TBMs. (A)** Scheme showing the experimental layout. **(B)** Representative flow cytometry plots showing CD169⁺ cells in inguinal LNs 7 d after NP-KLH immunization. Each dot represents a single mouse. *n* = 5 mice; two independent experiments. **(C and D)** Immunofluorescence staining of LNs derived from PBS- and DT-treated mice. **(E)** Quantification CD68⁺ cell density in GCs. Each dot represents a ratio in a single GC. *n* = 5 mice, two independent experiments. Line represents the mean. ***, P < 0.001; ns, not significant; two-tailed Student's *t* test.

number of TBMs in DT and PBS-treated mice (Fig. 4, D and E), demonstrating that CD169⁺ macrophages do not contribute to the TBM cell population.

TBMs in GCs show replenishment potential

GCs are long-lasting reactions that produce memory and plasma cells after the pathogen or vaccine regimen was cleared from the organism. To examine if GC macrophages can be replaced during the GC reaction, we used CX3CR1^{DTR} mice to ablate macrophages after the GCs were established. DT treatment of CX3CR1^{DTR} mice led to the depletion of CX3CR1⁺ macrophages from the PPs with a minimal effect on the presence of GC cells 5 d after the first DT injection, as assessed by flow cytometry and immunofluorescence (Fig. 5, A–C). Similar analysis of GC structures after an additional 7 d, revealed a similar number of CD68⁺ macrophages within GCs as observed prior to their depletion (Fig. 5 B). To examine if a similar effect occurs in vaccinated mice, we examined the inguinal LNs of immunized animals treated with DT. Although flow cytometry analysis revealed effective depletion of macrophages, immunofluorescence imaging revealed a significant number of residual TBMs in inguinal LNs in mice treated with DT (Fig. 5 D). This problem was previously reported in attempts to ablate TZMs in several mouse models (Baratin et al., 2017). Nonetheless, a similar trend of reduction in the density of TBMs in DT-treated mice followed by an increase in their frequency after an additional 9 d was observed (Fig. 5 D). We could not assess the long-term effects of macrophage depletion on GC functions since the DT treatment of CX3CR1^{DTR} mice triggered considerable side effects and was incomplete in some of the animals. Collectively, we conclude that TBMs are endowed with the potential to replenish their population during the GC reaction.

The final stage of B cell apoptosis in GCs occurs within TBMs

The major role of the TBM is to clear apoptotic B cells from the GC structures. However, it is not clear at which stage of their apoptotic process the B cells are removed by TBMs. To address this question, we stained LN sections with antibodies that detect caspase 3 activation events in B cells and performed terminal deoxynucleotidyl transferase dUTP nick end labeling (TUNEL) staining, which detects DNA fragmentation at the final stages of cell death. This analysis revealed that most of the activated caspase signals are not detected in TBMs, suggesting that the majority of the GC B cells initiate the apoptotic process before engulfment by TBM (Fig. 6 A). In contrast, TUNEL staining was only observed within TBM, suggesting that the final stage of cell death occurs after B cell engulfment by these cells (Fig. 6 A). To strengthen this conclusion, we used CX3CR1^{DTR} mice to ablate macrophages followed by in situ staining for apoptosis markers. Analysis of DT-treated mice revealed an increase in activated

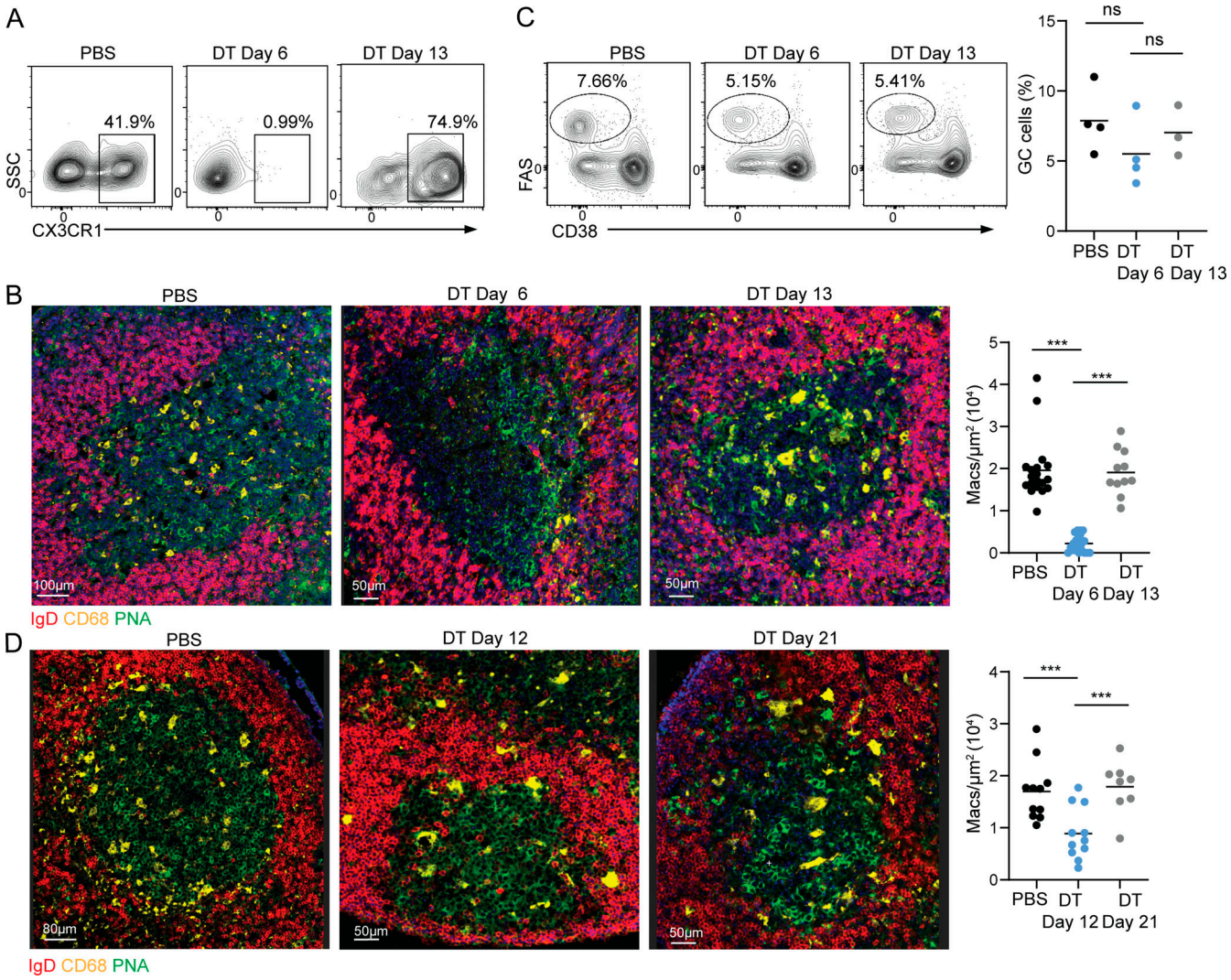

Figure 5. **TBMs in GCs are replaceable. (A)** Mice were treated with PBS or DT for every second day for 5 d, followed by 7 additional recovery days. Representative flow cytometry plots showing CX3CR1⁺ cells in PPs. **(B)** Immunofluorescence staining and quantification of PP CD68⁺ macrophages in GCs. Each dot represents an individual GC; three to four mice per condition in three experiments. **(C)** GC B cells in PBS-treated and DT-treated mice; three to four mice per condition in three experiments. Each dot represents a mouse. **(D)** Immunofluorescence staining of inguinal LNs derived from PBS or DT-treated mice at the indicated time points after the initial immunization. Each dot represents a GC. Data were collected from three independent experiments; three to four mice were used in each experiment. ***, P < 0.001; ns, not significant; one-way ANOVA.

caspase 3 signal within the GCs, and fragmented DNA was detected throughout the GC structure (Fig. 6, B and C). These observations demonstrate that B cells in GCs are removed through an efferocytosis process in which TBMs remove intact B cells at early apoptotic stages. Nonetheless, although our imaging approach was unable to detect cellular debris clearly, the removal of fragmented cells by TBM must occur as well (Allen et al., 2007; Mayer et al., 2017). Thus, the role of the TBMs is to minimize the accumulation of self-antigens and cellular debris in the extracellular space by limiting the dissemination of intracellular material.

Discussion

TBMs are among the last subtype of GC-resident cells whose cellular dynamics and precursors remain unknown. Previous studies used intravital imaging to demonstrate that lymphocytes constantly scan for cognate antigens through their rapid movement within lymphoid organs and in GCs, where cognate T–B interactions are critical for the antibody affinity maturation process (Shulman et al., 2014; Allen et al., 2007; Hauser et al., 2007b; Hauser et al., 2007a; Schwickert et al., 2007; Qi et al., 2008). Here, we show that in contrast to the scanning activity of lymphocytes, the TBMs take an approach of "stand hunting" in which the cells are stationary and await their prey to enter their proximity. This scavenging strategy is facilitated by the highly dynamic dendrites of the TBMs, which specifically recognize apoptotic B cells within the GC structures. TBMs are able to distinguish between GC B cells and other GC-resident cells, such as naive B cells and Tfh cells, suggesting that receptors expressed on the TBM dendrites can detect specific cell types based on "find me" and "eat me" signals located on the

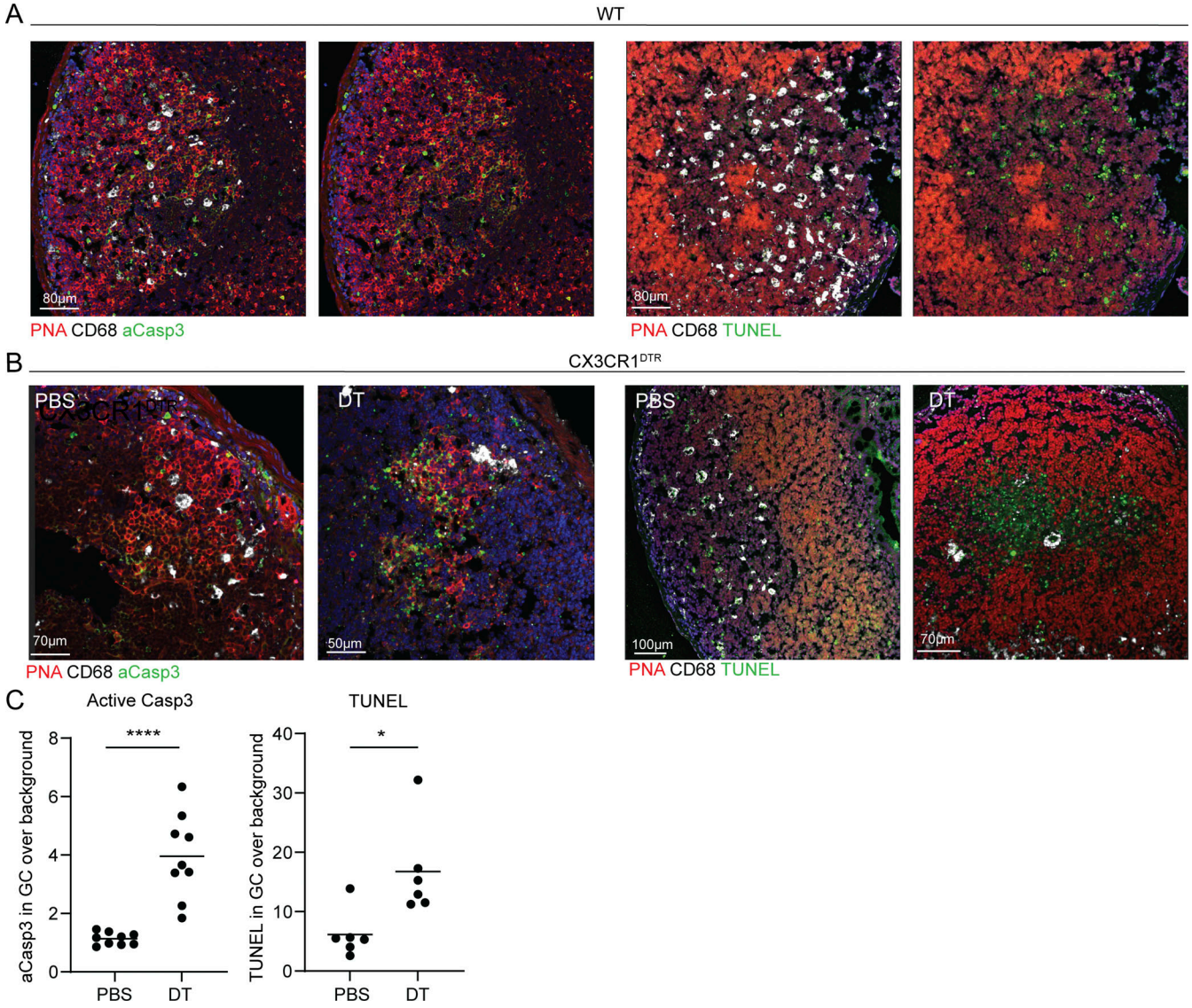

Figure 6. **TBMs accommodate the final stages of B cell apoptosis. (A)** Immunofluorescence staining for activated caspase 3 (aCasp3) and TUNEL of PPs derived from WT mice. **(B)** Immunofluorescence staining for activated caspase 3 and TUNEL in PPs derived from PBS or DT-treated CX3CR1^{DTR} mice. **(C)** Quantification of GC to background ratio of active caspase 3 and TUNEL signals. Each dot represents a GC. Data were collected from three mice in two independent experiments. Line represents the mean. *, P < 0.05; ***, P < 0.001; ns, not significant; two-tailed Student's *t* test.

surface of GC B cells (Ravichandran and Lorenz, 2007; Lemke, 2019). It is most likely that this cell-recognition event is mediated through the direct binding of PS or PS-binding adaptors on GC B cells by TBMs (Elliott et al., 2006; Bratton and Henson, 2008).

Using in silico modeling of GC dynamics, we suggest that 30 TBM cells are required for the removal of all of the apoptotic cells from a single GC, whereas our intervital measurements demonstrated that each GC hosts 25 TBM on average. This result is strikingly consistent with a measurement that was performed using alternate serial sections and histochemistry (Smith et al., 1991). Thus, a residual level of 10% apoptotic cells is predicted to remain in the GC structure at the peak of the response. Since TBMs are primarily located in the DZ of the GC, the number of residual apoptotic cells in this compartment is expected to be even smaller than our in silico estimation. Indeed previous measurements using reporter mice showed that 5% of the total population of apoptotic cells are not associated with TBMs in the DZ of the GC (Mayer et al., 2017), and an additional study reported 3% apoptotic cells in the DZ using flow cytometry (Stewart et al., 2018). Thus, our dynamic measurements and mathematical modeling suggest that TBMs efficiently remove nearly all the dying cells from the GC niche.

In unimmunized mice, most of the cortex-resident macrophages are located either in the T zone or within the subcapsular sinus, and very few macrophages are detected within the follicles (Bellomo et al., 2018). Time course imaging and experiments in GC-deficient mice revealed that few macrophages enter the follicles in a GC-dependent manner, suggesting that GC B cells attract this myeloid population (Smith et al., 1991). Although the GC structures are very close to the LN capsule where

SSMs reside (Moran et al., 2019), ablation experiments showed that follicular macrophages, specifically TBMs, do not arise from this cell subset. Furthermore, experiments using upper body–shielded chimeric mice demonstrated that BM-derived macrophages are not actively recruited to the LN follicles during the immune response. Since the chimeric mice were examined several weeks after the BM transplantation, our results suggest that the TBM precursors which reside in the LNs are long-lived cells. Yet, in fully irradiated mice, TBMs similar to TZMs, originated from the donor BM, suggesting that TBM precursors are monocyte-derived cells that reside in lymphoid organs for long periods. Most types of macrophages are long-lived cells (Perdiguero and Geissmann, 2016; Park et al., 2022), including TZMs that remove apoptotic cells and express shared surface molecules with TBMs, such as MERTK and CD68 (Bellomo et al., 2018). Furthermore, both TZMs and TBMs dispose of apoptotic cells through an efferocytosis process. These similarities are in favor of a model in which long-lived TZM gives rise to TBMs during a transient or chronic GC response through local proliferation and invasion into the LN follicles (Baratin et al., 2017). Furthermore, the lack of effect on TBMs following the ablation of the SSM also supports a TZM origin. We show that TBMs can be replenished over time which indicates that TZM-derived cells may replace exhausted TBMs in long-lasting GC reactions.

In GC reaction, a process that involves mutation-driven changes in immunoglobulin binding, disposal of intact apoptotic cells reduces the possibility of B cell interaction with intracellular self-antigens and antigenic spread by preventing the dissemination of intracellular self-material and cell blebs within the GC. We and others demonstrated that while caspase 3 activity is triggered outside the TBMs, the final stages of B cell apoptosis occur within the macrophage phagosome, suggesting that B cells are consumed before they complete the apoptosis process (Mayer et al., 2017; Kennedy et al., 2020). This mode of dead cell disposal minimizes the accumulation of cellular debris that may subvert the immune response (Martin et al., 2014). In addition, TBM-mediated cell disposal by efferocytosis also prevents the deposition of intracellular material on FDCs through complement receptors (Degn et al., 2017; Carroll, 2000; Mevorach et al., 1998). Thus, in addition to "cleaning up the GC" from cellular debris of dying cells (Allen et al., 2007; Mayer et al., 2017), an additional major function of the GC macrophages is to prevent the spreading of intracellular material in the GC microenvironment that might be recognized by mutated GC B cells during their interactions with the FDCs. Indeed, several studies suggest that a lack of effective TBM-mediated B cell uptake might be linked to the triggering of antibody-driven autoimmune diseases (Nagata et al., 2010; Asano et al., 2004; Hanayama et al., 2004; Cohen et al., 2002).

Although many subsets of innate cells have been defined by their transcriptome using single-cell RNA-sequencing approaches (Park et al., 2022), such analysis of TBMs is still impossible. Since these cells are very rare and difficult to extract from the LNs, our attempts to isolate or detect specific gene expression patterns of TBMs by RNA-sequencing methods have all failed. Indeed, TZM cells, which are significantly more abundant, are extremely difficult to extract from LNs (Baratin et al., 2017). Furthermore, since there is no genetic model to ablate GC macrophages specifically, since the existing ones such as CD11C^{DTR} and CX3CR1^{DTR} do not deplete LN macrophages effectively (Baratin et al., 2017), and since the mice suffer from severe side effects upon long-term DT treatment, it was not possible to study the long-lasting consequences of TBM depletion on the GC reaction.

TBM abundance and functions have been linked to the emergence of autoimmune diseases. The present study adds new insights into their origin and function, which may translate to a better understanding of the break of tolerance and the emergence of poly- and self-reactive antibodies in autoimmune pathologies and the emergence of autoantibodies in infectious disease and cancer (Mazor et al., 2022; Bastard et al., 2020; Nagata et al., 2010; Rahman et al., 2010).

Materials and methods

Mice

CX3CR1^{GFP}, CX3CR1^{DTR}, and CD169^{DTR} mice were kindly provided by Prof. Steffen Jung (Weizmann Institute of Science, Rehovot, Israel). SAP^{ko} mice were provided by Prof. Idit Shachar (Weizmann Institute of Science, Rehovot, Israel). OT-II and TdTomato^{+} mice were provided by the Jackson Laboratory. B1-8^{hi} B cells were previously described (Shih et al., 2002). WT mice (C57BL/6) were purchased from Envigo. Males and females between the ages of 8 and 12 wk at the start of the experiment were used. Mice were bred and housed under specific pathogen–free conditions. Animal handling protocols were approved by the Weizmann Institute Animal Care and Use Committee.

Chimeric mice

Chimeric mice were generated by irradiating host mice with 950 rad, followed by injection of fresh BM cells. Shielded chimeras were generated by covering the upper torso of the mice using a lead shield. Experiments with chimeric mice were performed 8 wk after BM transplantation.

Immunizations and DT treatments

NP-KLH (BioSearch Technologies) was prepared with alum and PBS at a final concentration of 0.4 mg/ml. Mice received a single administration of 25 µl (10 µg NP-KLH) into each footpad. In some experiments in which inguinal LNs were analyzed, the mice were immunized with 10 µl (50 µg NP-KLH) i.p. For imaging experiments, a prime-boost protocol was used as previously described (Shulman et al., 2014). Host mice were primed i.p. with OVA in alum followed by boosting with soluble NP-OVA, which was injected into the upper part of the footpad after at least 14 d. Where indicated, mice received three injections of 600 ng DT (CX3CR1^{DTR} mice) or three injections of 400 ng DT (CD169^{DTR} mice) as described in the figure legends.

Adoptive cell transfers

TdTomato^{+} B1-8^{hi} B cells and OT-II T cells were purified by forcing spleen tissue through mesh into PBS or RPMI containing 2% serum and 1 mM EDTA. Resting B cells and T cells were

purified using anti-CD43 magnetic beads or CD4+ T cell–negative isolation kits (Miltenyi), respectively. After purification, 3–4 × 10^6 B1-8^{hi} (comprising 15% Igλ+ NP-specific B cells) before boosting with NP-OVA or 1 × 10^5 OT-II T cells were transferred intravenously into $CX3CR1^{GFP}$ before initial OVA immunization. In Fig. 1 D, naive B cells were transferred into mice on day 6 after boosting with NP-OVA.

Intravital imaging by TPLSM

Host mice were anesthetized with a mixture of 50 mg ketamine, 15 mg xylazine, and 2.5 mg acepromazine per kg of body weight and maintained under anesthesia by inhalation of 1% isofluorane. Hind legs were shaved and placed on a stage heated to 37°C. Popliteal LNs were surgically exposed, immobilized, covered with a coverslip, and placed under the microscope objective (Zeiss 20 Å~1.05-NA plan objective). A Zeiss LSM 880 upright microscope fitted with Coherent Chameleon Vision laser was used for whole LN scan imaging experiments. Images were acquired with a femtosecond-pulsed two-photon laser tuned to 900–940 nm. The microscope was fitted with a 565 LPXR filter cube to split the emission to a PMT detector (with a 579–631 nm filter for tdTomato fluorescence), and an additional 505 LPXR mirror to further split the emission to two GaAsp detectors (with a 500–550 nm filter for GFP fluorescence). The zoom was set to 0.7 and images were acquired at 512 × 512 x-y resolution.

Flow cytometry

LNs were removed, washed in cold PBS, and forced through a mesh into PBS containing 2% FCS and 1 mM EDTA to create single-cell suspensions. Cell suspensions from PPs were similarly prepared by excising PPs from sections of small intestines prewashed with ice-cold PBS to remove fecal content. To block Fc receptors, washed cells were incubated with 2 µg/ml anti-16/32 (TruStain FcX, BioLegend) for 5–10 min before antibody staining. Cells were subsequently incubated with fluorescently labeled antibodies for 30 min on ice. GC cells were gated as live/single, B220+ (clone RA3-6B2; BioLegend) CD38− (clone 90; Invitrogen) FAS+ (clone Jo2; BD Bioscience). SSMs were gated as CD169+ (clone 3D6.112; BioLegend), and total monocytes and macrophages were gated as CX3CR1+ cells (clone SA011F11; BioLegend). Stained cell suspensions were analyzed using a CytoFlex flow cytometer (Beckman Coulter).

Cryosections and immunofluorescence staining

LNs were taken directly for PBS wash, then fixed in 4% paraformaldehyde for 2 h at room temperature. The LNs were then transferred to 30% sucrose solution overnight at 4°C for 2 consecutive days. The LNs were transferred into designated molds on dry ice and submerged in optimal cutting temperature compound for embedding. The blocks were kept at −80°C until cut. Sections of 7–9 µm thickness were cut by a cryostat and then transferred to glass slides to evenly spread the sections. The tissues were fixed in acetone for 7 min at −20°C and then rehydrated with PBS. To enable staining, the slides were treated with 1% SDS for 10 min at room temperature followed by washing the remaining residues. The slides were submerged in 5% BSA in PBS containing 0.05% TWEEN for 1 h at room temperature before staining with fluorescently labeled antibodies overnight at 4°C IgD-PE (clone 11-26c.2a; BioLegend), CD68-Alexa Fluor 647 (clone FA-11; BioLegend), PNA-Alexa Fluor 488 (Invitrogen), CD169 Alexa Fluor 647 (clone 3D6.112; BioLegend), cleaved caspase 3 (D175; Cell Signaling), and goat anti-rabbit Alexa Fluor 488 (Abcam). The following day, cell nuclei were stained with Hoechst for 5 min at room temperature and then washed and sealed with Immunomount (Bar Naor Ltd). Immunofluorescence confocal microscopy was performed using a Zeiss LSM 880 confocal microscope.

TUNEL staining

LNs were fixed and embedded as described above. 5-µm sections were placed on slides and fixed in 4% paraformaldehyde in 1% TBS for 20 min, then washed with TBS for 30 min. Permeabilization was done using Triton 0.1% in TBS FOR 5 min and then washed with TBS. The slides were incubated with the TUNEL mix (Invitrogen) for 1 h at 37°C. The slides were washed with TBS before staining with anti-BrdU AF-488 for 30 min at room temperature. Propidium iodide was added to the slides for 15 min at room temperature prior to TBS wash. The slides were submerged in blocking solution, as described, and stained with IgD-PE (clone 11-26c.2a) or PNA Alexa Fluor 594 (Invitrogen) and CD68 Alexa Fluor 647 (clone FA-11; BioLegend) overnight at 4°C.

Statistical analysis and reproducibility

Statistical significance was determined using GraphPad Prism v7.0 with the tests indicated in each figure.

Mathematical modeling of TBMs and apoptotic GC B cells

An agent-based model in which every B cell has its own kinetics and probability of undergoing apoptosis was implemented to study the efficiency of clearance of apoptotic B cells using different numbers of TBMs and their uptake rates (Meyer-Hermann, 2021). The probability of a given B cell undergoing apoptosis was considered to be dependent on T cell help. Two different algorithms for removing the apoptotic B cells from the GC were examined. In the first approach, the apoptotic B cells were removed from the GC with a given predefined probability (assigned on the basis of the uptake rate and number of TBMs) at each time step of the simulation. In the second approach, TBMs were explicitly introduced into the model as distinct agents. Apoptotic B cells could be phagocytosed by a TBM if the TBM had not previously phagocytosed a B cell within a predefined time window. While the spatial distribution was not taken into account in the first approach, in the second algorithm, TBMs were assumed to be static, isolated from each other, and distributed randomly in the LZ. Further, TBMs were assigned constant uptake rates and vicinities within which they could phagocytose B cells. Both methods yielded comparable results for the maximum number of residual apoptotic B cells. More details describing the simulation framework and related parameters in these simulations can be found in Meyer-Hermann (2021).

Online supplemental material

Video 1 shows that TBMs are stationary cells that interact with GC B cells through dynamic protrusions. Video 2, Video 3, and Video 4 demonstrate that TBMs use dendrites to scavenge GC B cells.

Acknowledgments

Z. Shulman is supported by European Research Council grant no. 101001613, Israel Science Foundation grant no. 1090/18, and the Morris Kahn Institute for Human Immunology. Z. Shulman is a member of the European Molecular Biology Organization Young Investigator Program. Z. Shulman is supported by grants from the Azrieli Foundation, the Moross Integrated Cancer Center, and Miel de Botton. N. Schwan has received funding from the Innovative Medicines Initiative 2 Joint Undertaking under grant agreement no. 101007799. The Joint Undertaking receives support from the European Union's Horizon 2020 research and innovation program and European Federation of Pharmaceutical Industries and Associations.

Author contributions: N. Gurwicz: Conceptualization, data curation, formal analysis, investigation, visualization, writing—original draft and review. L. Stoler-Barak: Data curation, formal analysis, methodology. N. Schwan, A. Bandyopadhyay, and M. Meyer-Hermann: Computational analysis of GC B cell uptake by macrophages. Z. Shulman: Conceptualization, funding acquisition, project administration, supervision, validation, and writing of the manuscript.

Disclosures: The authors declare no competing interests exist.

Submitted: 20 December 2022
Revised: 10 January 2023
Accepted: 11 January 2023

References

Allen, C.D.C., K.M. Ansel, C. Low, R. Lesley, H. Tamamura, N. Fujii, and J.G. Cyster. 2004. Germinal center dark and light zone organization is mediated by CXCR4 and CXCR5. *Nat. Immunol.* 5:943–952. https://doi.org/10.1038/ni1100

Allen, C.D.C., T. Okada, H.L. Tang, and J.G. Cyster. 2007. Imaging of germinal center selection events during affinity maturation. *Science*. 315:528–531. https://doi.org/10.1126/science.1136736

Asano, K., M. Miwa, K. Miwa, R. Hanayama, H. Nagase, S. Nagata, and M. Tanaka. 2004. Masking of phosphatidylserine inhibits apoptotic cell engulfment and induces autoantibody production in mice. *J. Exp. Med.* 200:459–467. https://doi.org/10.1084/jem.20040342

Baratin, M., L. Simon, A. Jorquera, C. Ghigo, D. Dembele, J. Nowak, R. Gentek, S. Wienert, F. Klauschen, B. Malissen, et al. 2017. T cell zone resident macrophages silently dispose of apoptotic cells in the lymph node. *Immunity*. 47:349–362.e5. https://doi.org/10.1016/j.immuni.2017.07.019

Bastard, P., L.B. Rosen, Q. Zhang, E. Michailidis, H.-H. Hoffmann, Y. Zhang, K. Dorgham, Q. Philippot, J. Rosain, V. Béziat, et al. 2020. Autoantibodies against type I IFNs in patients with life-threatening COVID-19. *Science*. 370:eabd4585 https://doi.org/10.1126/science.abd4585

Baumann, I., W. Kolowos, R.E. Voll, B. Manger, U. Gaipl, W.L. Neuhuber, T. Kirchner, J.R. Kalden, and M. Herrmann. 2002. Impaired uptake of apoptotic cells into tingible body macrophages in germinal centers of patients with systemic lupus erythematosus. *Arthritis Rheum.* 46: 191–201. https://doi.org/10.1002/1529-0131(200201)46:1<191::AID-ART10027>3.0.CO;2-K

Bellomo, A., R. Gentek, M. Bajénoff, and M. Baratin. 2018. Lymph node macrophages: Scavengers, immune sentinels and trophic effectors. *Cell. Immunol.* 330:168–174. https://doi.org/10.1016/j.cellimm.2018.01.010

Bellomo, A., R. Gentek, R. Golub, and M. Bajénoff. 2021. Macrophage-fibroblast circuits in the spleen. *Immunol. Rev.* 302:104–125. https://doi.org/10.1111/imr.12979

Biram, A., and Z. Shulman. 2020. T cell help to B cells: Cognate and atypical interactions in peripheral and intestinal lymphoid tissues. *Immunol. Rev.* 296:36–47. https://doi.org/10.1111/imr.12890

Biram, A., E. Winter, A.E. Denton, I. Zaretsky, B. Dassa, M. Bemark, M.A. Linterman, G. Yaari, and Z. Shulman. 2020. B cell diversification is uncoupled from SAP-mediated selection forces in chronic germinal centers within peyer's patches. *Cell Rep.* 30:1910–1922.e5. https://doi.org/10.1016/j.celrep.2020.01.032

Bratton, D.L., and P.M. Henson. 2008. Apoptotic cell recognition: Will the real phosphatidylserine receptor(s) please stand up? *Curr. Biol.* 18:R76–R79. https://doi.org/10.1016/j.cub.2007.11.024

Cannons, J.L., S.G. Tangye, and P.L. Schwartzberg. 2011. SLAM family receptors and SAP adaptors in immunity. *Annu. Rev. Immunol.* 29:665–705. https://doi.org/10.1146/annurev-immunol-030409-101302

Carrasco, Y.R., and F.D. Batista. 2007. B cells acquire particulate antigen in a macrophage-rich area at the boundary between the follicle and the subcapsular sinus of the lymph node. *Immunity*. 27:160–171. https://doi.org/10.1016/j.immuni.2007.06.007

Carroll, M.C. 2000. The role of complement in B cell activation and tolerance. *Adv. Immunol.* 74:61–88. https://doi.org/10.1016/S0065-2776(08)60908-6

Cohen, P.L., R. Caricchio, V. Abraham, T.D. Camenisch, J.C. Jennette, R.A.S. Roubey, H.S. Earp, G. Matsushima, and E.A. Reap. 2002. Delayed apoptotic cell clearance and lupus-like autoimmunity in mice lacking the c-mer membrane tyrosine kinase. *J. Exp. Med.* 196:135–140. https://doi.org/10.1084/jem.20012094

Crotty, S., E.N. Kersh, J. Cannons, P.L. Schwartzberg, and R. Ahmed. 2003. SAP is required for generating long-term humoral immunity. *Nature*. 421:282–287. https://doi.org/10.1038/nature01318

de Carvalho, R.V.H., J. Ersching, A. Barbulescu, A. Hobbs, T.B.R. Castro, L. Mesin, J.T. Jacobsen, B.K. Phillips, H.-H. Hoffmann, R. Parsa, et al. 2022. Clonal replacement sustains long-lived germinal centers primed by respiratory viruses. *Cell*. https://doi.org/10.1016/j.cell.2022.11.031

Degn, S.E., C.E. van der Poel, D.J. Firl, B. Ayoglu, F.A. Al Qureshah, G. Bajic, L. Mesin, C.-A. Reynaud, J.-C. Weill, P.J. Utz, et al. 2017. Clonal evolution of autoreactive germinal centers. *Cell*. 170:913–926.e19. https://doi.org/10.1016/j.cell.2017.07.026

Elliott, J.I., A. Sardini, J.C. Cooper, D.R. Alexander, S. Davanture, G. Chimini, and C.F. Higgins. 2006. Phosphatidylserine exposure in B lymphocytes: A role for lipid packing. *Blood*. 108:1611–1617. https://doi.org/10.1182/blood-2005-11-012328

Flemming, W. 1884. Studien über Regeneration der Gewebe. *Archiv für mikroskopische Anatomie*. 24:50–91

Gaipl, U.S., R.E. Voll, A. Sheriff, S. Franz, J.R. Kalden, and M. Herrmann. 2005. Impaired clearance of dying cells in systemic lupus erythematosus. *Autoimmun. Rev.* 4:189–194. https://doi.org/10.1016/j.autrev.2004.10.007

Glaros, V., R. Rauschmeier, A.V. Artemov, A. Reinhardt, S. Ols, A. Emmanouilidi, C. Gustafsson, Y. You, C. Mirabello, Å.K. Björklund, et al. 2021. Limited access to antigen drives generation of early B cell memory while restraining the plasmablast response. *Immunity*. 54: 2005–2023.e10. https://doi.org/10.1016/j.immuni.2021.08.017

Gray, E.E., and J.G. Cyster. 2012. Lymph node macrophages. *J. Innate Immun.* 4:424–436. https://doi.org/10.1159/000337007

Grenov, A., H. Hezroni, L. Lasman, J.H. Hanna, and Z. Shulman. 2022. YTHDF2 suppresses the plasmablast genetic program and promotes germinal center formation. *Cell Rep.* 39:110778. https://doi.org/10.1016/j.celrep.2022.110778

Guilliams, M., G.R. Thierry, J. Bonnardel, and M. Bajenoff. 2020. Establishment and maintenance of the macrophage niche. *Immunity*. 52:434–451. https://doi.org/10.1016/j.immuni.2020.02.015

Hägglöf, T., M. Cipolla, M. Loewe, S.T. Chen, L. Mesin, H. Hartweger, M.A. ElTanbouly, A. Cho, A. Gazumyan, V. Ramos, et al. 2022. Continuous germinal center invasion contributes to the diversity of the immune response. *Cell*. https://doi.org/10.1016/j.cell.2022.11.032

Hanayama, R., M. Tanaka, K. Miyasaka, K. Aozasa, M. Koike, Y. Uchiyama, and S. Nagata. 2004. Autoimmune disease and impaired uptake of apoptotic cells in MFG-E8-deficient mice. *Science*. 304:1147–1150. https://doi.org/10.1126/science.1094359

Hasham, M.G., K.J. Snow, N.M. Donghia, J.A. Branca, M.D. Lessard, J. Stavnezer, L.S. Shopland, and K.D. Mills. 2012. Activation-induced cytidine deaminase-initiated off-target DNA breaks are detected and resolved during S phase. *J. Immunol.* 189:2374–2382. https://doi.org/10.4049/jimmunol.1200414

Hauser, A.E., T. Junt, T.R. Mempel, M.W. Sneddon, S.H. Kleinstein, S.E. Henrickson, U.H. von Andrian, M.J. Shlomchik, and A.M. Haberman. 2007a. Definition of germinal-center B cell migration in vivo reveals

predominant intrazonal circulation patterns. *Immunity* 26:655–667. https://doi.org/10.1016/j.immuni.2007.04.008

Hauser, A.E., M.J. Shlomchik, and A.M. Haberman. 2007b. In vivo imaging studies shed light on germinal-centre development. *Nat. Rev. Immunol.* 7:499–504. https://doi.org/10.1038/nri2120

Hofman, F.M., D. Lopez, L. Husmann, P.R. Meyer, and C.R. Taylor. 1984. Heterogeneity of macrophage populations in human lymphoid tissue and peripheral blood. *Cell. Immunol.* 88:61–74. https://doi.org/10.1016/0008-8749(84)90052-2

Jung, S., J. Aliberti, P. Graemmel, M.J. Sunshine, G.W. Kreutzberg, A. Sher, and D.R. Littman. 2000. Analysis of fractalkine receptor CX(3)CR1 function by targeted deletion and green fluorescent protein reporter gene insertion. *Mol. Cell. Biol.* 20:4106–4114. https://doi.org/10.1128/MCB.20.11.4106-4114.2000

Kennedy, D.E., M.K. Okoreeh, M. Maienschein-Cline, J. Ai, M. Veselits, K.C. McLean, Y. Dhungana, H. Wang, J. Peng, H. Chi, et al. 2020. Novel specialized cell state and spatial compartments within the germinal center. *Nat. Immunol.* 21:660–670. https://doi.org/10.1038/s41590-020-0660-2

Khan, T.N., E.B. Wong, C. Soni, and Z.S.M. Rahman. 2013. Prolonged apoptotic cell accumulation in germinal centers of Mer-deficient mice causes elevated B cell and $CD4^+$ Th cell responses leading to autoantibody production. *J. Immunol.* 190:1433–1446. https://doi.org/10.4049/jimmunol.1200824

Kranich, J., N.J. Krautler, E. Heinen, M. Polymenidou, C. Bridel, A. Schildknecht, C. Huber, M.H. Kosco-Vilbois, R. Zinkernagel, G. Miele, et al. 2008. Follicular dendritic cells control engulfment of apoptotic bodies by secreting Mfge8. *J. Exp. Med.* 205:1293–1302. https://doi.org/10.1084/jem.20071019

Lemke, G. 2019. How macrophages deal with death. *Nat. Rev. Immunol.* 19:539–549. https://doi.org/10.1038/s41577-019-0167-y

Liu, Y.J., D.E. Joshua, G.T. Williams, C.A. Smith, J. Gordon, and I.C. MacLennan. 1989. Mechanism of antigen-driven selection in germinal centres. *Nature.* 342:929–931. https://doi.org/10.1038/342929a0

Liu, Y.J., D.Y. Mason, G.D. Johnson, and S. Abbot. 1991. Germinal center cells express bcl-2 protein after activation by signals which prevent their entry into apoptosis. *Eur J. Immunol.* 21:1905–1910. https://doi.org/10.1002/eji.1830210819

Ma, C.S., S. Pittaluga, D.T. Avery, N.J. Hare, I. Maric, A.D. Klion, K.E. Nichols, and S.G. Tangye. 2006. Selective generation of functional somatically mutated IgM+CD27+, but not Ig isotype-switched, memory B cells in X-linked lymphoproliferative disease. *J. Clin. Invest.* 116:322–333. https://doi.org/10.1172/JCI25720

Martin, C.J., K.N. Peters, and S.M. Behar. 2014. Macrophages clean up: Efferocytosis and microbial control. *Curr. Opin. Microbiol.* 17:17–23. https://doi.org/10.1016/j.mib.2013.10.007

Mayer, C.T., A. Gazumyan, E.E. Kara, A.D. Gitlin, J. Golijanin, C. Viant, J. Pai, T.Y. Oliveira, Q. Wang, A. Escolano, et al. 2017. The microanatomic segregation of selection by apoptosis in the germinal center. *Science.* 358:eaao2602. https://doi.org/10.1126/science.aao2602

Mazor, R.D., N. Nathan, A. Gilboa, L. Stoler-Barak, L. Moss, I. Solomonov, A. Hanuna, Y. Divinsky, M.D. Shmueli, H. Hezroni, et al. 2022. Tumor-reactive antibodies evolve from non-binding and autoreactive precursors. *Cell.* 185:1208–1222.e21. https://doi.org/10.1016/j.cell.2022.02.012

Mevorach, D., J.O. Mascarenhas, D. Gershov, and K.B. Elkon. 1998. Complement-dependent clearance of apoptotic cells by human macrophages. *J. Exp. Med.* 188:2313–2320. https://doi.org/10.1084/jem.188.12.2313

Meyer-Hermann, M. 2021. A molecular theory of germinal center B cell selection and division. *Cell Rep.* 36:109552. https://doi.org/10.1016/j.celrep.2021.109552

Mondor, I., M. Baratin, M. Lagueyrie, L. Saro, S. Henri, R. Gentek, D. Suerinck, W. Kastenmuller, J.X. Jiang, and M. Bajénoff. 2019. Lymphatic endothelial cells are essential components of the subcapsular sinus macrophage niche. *Immunity.* 50:1453–1466.e4. https://doi.org/10.1016/j.immuni.2019.04.002

Moran, I., A.K. Grootveld, A. Nguyen, and T.G. Phan. 2019. Subcapsular sinus macrophages: The seat of innate and adaptive memory in murine lymph nodes. *Trends Immunol.* 40:35–48. https://doi.org/10.1016/j.it.2018.11.004

Muramatsu, M., K. Kinoshita, S. Fagarasan, S. Yamada, Y. Shinkai, and T. Honjo. 2000. Class switch recombination and hypermutation require activation-induced cytidine deaminase (AID), a potential RNA editing enzyme. *Cell.* 102:553–563. https://doi.org/10.1016/S0092-8674(00)00078-7

Nagata, S., R. Hanayama, and K. Kawane. 2010. Autoimmunity and the clearance of dead cells. *Cell.* 140:619–630. https://doi.org/10.1016/j.cell.2010.02.014

Park, M.D., A. Silvin, F. Ginhoux, and M. Merad. 2022. Macrophages in health and disease. *Cell.* 185:4259–4279. https://doi.org/10.1016/j.cell.2022.10.007

Peperzak, V., I.B. Vikstrom, and D.M. Tarlinton. 2012. Through a glass less darkly: Apoptosis and the germinal center response to antigen. *Immunol. Rev.* 247:93–106. https://doi.org/10.1111/j.1600-065X.2012.01123.x

Perdiguero, E.G., and F. Geissmann. 2016. The development and maintenance of resident macrophages. *Nat. Immunol.* 17:2–8. https://doi.org/10.1038/ni.3341

Phan, T.G., I. Grigorova, T. Okada, and J.G. Cyster. 2007. Subcapsular encounter and complement-dependent transport of immune complexes by lymph node B cells. *Nat. Immunol.* 8:992–1000. https://doi.org/10.1038/ni1494

Phan, T.G., J.A. Green, E.E. Gray, Y. Xu, and J.G. Cyster. 2009. Immune complex relay by subcapsular sinus macrophages and noncognate B cells drives antibody affinity maturation. *Nat. Immunol.* 10:786–793. https://doi.org/10.1038/ni.1745

Qi, H., J.L. Cannons, F. Klauschen, P.L. Schwartzberg, and R.N. Germain. 2008. SAP-controlled T-B cell interactions underlie germinal centre formation. *Nature.* 455:764–769. https://doi.org/10.1038/nature07345

Rabinowitz, S.S., and S. Gordon. 1991. Macrosialin, a macrophage-restricted membrane sialoprotein differentially glycosylated in response to inflammatory stimuli. *J. Exp. Med.* 174:827–836. https://doi.org/10.1084/jem.174.4.827

Rahman, Z.S.M., W.-H. Shao, T.N. Khan, Y. Zhen, and P.L. Cohen. 2010. Impaired apoptotic cell clearance in the germinal center by Mer-deficient tingible body macrophages leads to enhanced antibody-forming cell and germinal center responses. *J. Immunol.* 185:5859–5868. https://doi.org/10.4049/jimmunol.1001187

Ravichandran, K.S., and U. Lorenz. 2007. Engulfment of apoptotic cells: Signals for a good meal. *Nat. Rev. Immunol.* 7:964–974. https://doi.org/10.1038/nri2214

Savill, J., I. Dransfield, C. Gregory, and C. Haslett. 2002. A blast from the past: Clearance of apoptotic cells regulates immune responses. *Nat. Rev. Immunol.* 2:965–975. https://doi.org/10.1038/nri957

Schwickert, T.A., R.L. Lindquist, G. Shakhar, G. Livshits, D. Skokos, M.H. Kosco-Vilbois, M.L. Dustin, and M.C. Nussenzweig. 2007. In vivo imaging of germinal centres reveals a dynamic open structure. *Nature.* 446:83–87. https://doi.org/10.1038/nature05573

Schwickert, T.A., B. Alabyev, T. Manser, and M.C. Nussenzweig. 2009. Germinal center reutilization by newly activated B cells. *J. Exp. Med.* 206:2907–2914. https://doi.org/10.1084/jem.20091225

Shih, T.A., E. Meffre, M. Roederer, and M.C. Nussenzweig. 2002. Role of BCR affinity in T cell dependent antibody responses in vivo. *Nat. Immunol.* 3:570–575. https://doi.org/10.1038/ni803

Shlomchik, M.J., and F. Weisel. 2012. Germinal center selection and the development of memory B and plasma cells. *Immunol. Rev.* 247:52–63. https://doi.org/10.1111/j.1600-065X.2012.01124.x

Shulman, Z., A.D. Gitlin, S. Targ, M. Jankovic, G. Pasqual, M.C. Nussenzweig, and G.D. Victora. 2013. T follicular helper cell dynamics in germinal centers. *Science.* 341:673–677. https://doi.org/10.1126/science.1241680

Shulman, Z., A.D. Gitlin, J.S. Weinstein, B. Lainez, E. Esplugues, R.A. Flavell, J.E. Craft, and M.C. Nussenzweig. 2014. Dynamic signaling by T follicular helper cells during germinal center B cell selection. *Science.* 345:1058–1062. https://doi.org/10.1126/science.1257861

Sminia, T., M.M. Wilders, E.M. Janse, and E.C. Hoefsmit. 1983. Characterization of non-lymphoid cells in Peyer's patches of the rat. *Immunobiology.* 164:136–143. https://doi.org/10.1016/S0171-2985(83)80005-9

Smith, J.P., A.M. Lister, J.G. Tew, and A.K. Szakal. 1991. Kinetics of the tingible body macrophage response in mouse germinal center development and its depression with age. *Anat. Rec.* 229:511–520. https://doi.org/10.1002/ar.1092290412

Smith, J.P., G.F. Burton, J.G. Tew, and A.K. Szakal. 1998. Tingible body macrophages in regulation of germinal center reactions. *Dev. Immunol.* 6:285–294. https://doi.org/10.1155/1998/38923

Stewart, I., D. Radtke, B. Phillips, S.J. McGowan, and O. Bannard. 2018. Germinal center B cells replace their antigen receptors in dark zones and fail light zone entry when immunoglobulin gene mutations are damaging. *Immunity.* 49:477–489.e7. https://doi.org/10.1016/j.immuni.2018.08.025

Suan, D., A. Nguyen, I. Moran, K. Bourne, J.R. Hermes, M. Arshi, H.R. Hampton, M. Tomura, Y. Miwa, A.D. Kelleher, et al. 2015. T follicular helper cells have distinct modes of migration and molecular signatures in naive and memory immune responses. *Immunity*. 42:704–718. https://doi.org/10.1016/j.immuni.2015.03.002

Swartzendruber, D.C., and C.C. Congdon. 1963. Electron microscope observations on tingible body macrophages in mouse spleen. *J. Cell Biol.* 19: 641–646. https://doi.org/10.1083/jcb.19.3.641

Victora, G.D., and M.C. Nussenzweig. 2012. Germinal centers. *Annu. Rev. Immunol.* 30:429–457. https://doi.org/10.1146/annurev-immunol-020711-075032

Vinuesa, C.G., I. Sanz, and M.C. Cook. 2009. Dysregulation of germinal centres in autoimmune disease. *Nat. Rev. Immunol.* 9:845–857. https://doi.org/10.1038/nri2637

Wittenbrink, N., A. Klein, and A.A. Weiser, J. Schuchhardt, M. Or-Guil. 2011. Is there a typical germinal center? A large-scale immunohistological study on the cellular composition of germinal centers during the hapten-carrier–driven primary immune response in mice. *J. Immunol.* 187:6185–6196. https://doi.org/10.4049/jimmunol.1101440

Wong, K., P.A. Valdez, C. Tan, S. Yeh, J.-A. Hongo, and W. Ouyang. 2010. Phosphatidylserine receptor Tim-4 is essential for the maintenance of the homeostatic state of resident peritoneal macrophages. *Proc. Natl. Acad. Sci. USA*. 107:8712–8717. https://doi.org/10.1073/pnas.0910929107

Zaheen, A., and A. Martin. 2011. Activation-induced cytidine deaminase and aberrant germinal center selection in the development of humoral autoimmunities. *Am. J. Pathol.* 178:462–471. https://doi.org/10.1016/j.ajpath.2010.09.044

Supplemental material

Video 1. **TBMs are stationary cells that interact with GC B cells through dynamic protrusions.** CX3CR1^{GFP} were primed with OVA and after 14 d received tdTomato^{+} B1-8^{hi} B cells followed by injection with NP-OVA to the footpad. After an additional 7 d, the mice were subjected to intervital TPLSM. Green, macrophages; red, B cells.

Video 2. **TBMs use dendrites to scavenge GC B cells; example 1.** CX3CR1^{GFP} were primed with OVA and after 14 d received tdTomato^{+} B1-8^{hi} B cells followed by injection with NP-OVA to the footpad. After an additional 7 d, the mice were subjected to intervital TPLSM. Green, macrophages; red, B cells.

Video 3. **TBMs use dendrites to scavenge GC B cells; example 2.** CX3CR1^{GFP} were primed with OVA and after 14 d received tdTomato^{+} B1-8^{hi} B cells followed by injection with NP-OVA to the footpad. After an additional 7 d, the mice were subjected to intervital TPLSM. Green, macrophages; red, B cells.

Video 4. **TBMs use dendrites to scavenge GC B cells; example 3.** CX3CR1^{GFP} were primed with OVA and after 14 d received tdTomato^{+} B1-8^{hi} B cells followed by injection with NP-OVA to the footpad. After an additional 7 d, the mice were subjected to intervital TPLSM. Green, macrophages; red, B cells.